

and  $b_K=0.054 \mu^{-2}$ , the quantities  $R_1$  and  $R_2$  are 1.52 and 1.57, respectively.<sup>25</sup> The reasonable agreement of the branching ratios with the experiments in the linear approximation of the matrix element was shown by Bég<sup>26</sup> and Wali.<sup>27</sup>

### III. CONCLUSIONS

Treating  $\eta$  and  $K$  decays in a similar fashion (just interchanging  $\eta$  and  $K$  masses), we obtain good results

<sup>25</sup> Finally, we study the effects of low-energy  $S$ -wave  $I=2 \pi\pi$  interactions using experimental values of the phase shift ( $\delta_2^0 \sim -15^\circ$ ) given in Ref. 11. This raises the branching ratio by about 5% and the slope by about 4%.

<sup>26</sup> M. A. B. Bég, Phys. Rev. Letters **9**, 67 (1962).

<sup>27</sup> K. C. Wali, Phys. Rev. Letters **9**, 120 (1962).

for their branching ratios and their energy spectra. This shows that the final-state interactions dominate the decay structure. The interesting result obtained is that the  $\rho$  effects dominate the  $S$  in the slope. The slight deviation of the predicted spectrum from the experimental values may be due to retaining only linear terms in the matrix element.

### ACKNOWLEDGMENTS

The author is indebted to Professor S. N. Biswas for suggesting this problem and for many helpful discussions. He is also grateful to Dr. S. H. Patil for constant help and encouragement.

## Pion Production in the Proton-Deuteron Interaction

P. K. PATNAIK

Department of Physics, Indian Institute of Technology, Kanpur, India

(Received 26 February 1968; revised manuscript received 24 June 1968)

The differential cross section for the reaction  $p+d \rightarrow \text{He}^3 + \pi^0$  has been calculated taking Born diagrams alone. The form factor for the  $p d \text{He}^3$  vertex is obtained. The result is compared with the available experimental result and found to be in fair agreement.

### I. INTRODUCTION

RECENTLY, Melissinos and Dahanayake<sup>1</sup> have reported a measurement of the differential cross section for the reaction

$$p+d \rightarrow \text{He}^3 + \pi^0 \quad (1)$$

at proton laboratory kinetic energy  $T_p=1.515$  BeV and c.m. angle  $\theta_{c.m.}=0^\circ$ . They obtain

$$d\sigma/d\Omega = (4.1_{-2}^{+4}) \times 10^{-32} \text{ cm}^2.$$

Earlier, Harting *et al.*<sup>2</sup> observed the same reaction at  $T_p=600$  MeV and  $\theta_{c.m.}=52^\circ$ . Their result is

$$d\sigma/d\Omega = (6.1 \pm 2) \times 10^{-30} \text{ cm}^2.$$

Note that one result is a hundred times larger than the other one. This is essentially attributed<sup>1</sup> to the rapidly varying angular distribution that has been observed in other similar reactions.<sup>3</sup> To check this we have computed the differential cross section taking the Born diagrams (see Fig. 1). Our results also indicate rapid angular variation. Some time ago, Mathews and

Deo,<sup>4</sup> Heinz *et al.*,<sup>5</sup> and Deo and Patnaik<sup>6</sup> computed the differential cross section for the reaction  $p+p \rightarrow d+\pi^+$  with nucleon exchange and obtained many desirable results. We believe that a similar nucleon exchange also plays a dominant role in the reaction (1). However, there is another second-order diagram (Fig. 2) involving the  $\text{He}^3$  pole that is also important, particularly at lower energy. Here we report the results of our calculation with these two Feynman diagrams. We are aware of the fact that the nucleon is far away from the mass shell and that its contribution cannot be calculated

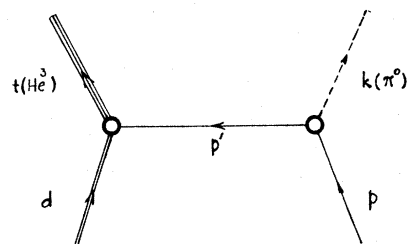


FIG. 1. Feynman diagram for single-proton exchange in  $p+d \rightarrow \text{He}^3 + \pi^0$ .

<sup>1</sup> A. C. Melissinos and C. Dahanayake, Phys. Rev. **159**, 1210 (1967).

<sup>2</sup> D. Harting, T. C. Kluyver, A. Kusumegi, R. Rigopoulos, A. M. Sachs, G. Tibebe, G. Vanderhaeghe, and G. Weber, Phys. Rev. Letters **3**, 52 (1959).

<sup>3</sup> O. E. Overseth, R. Heinz, L. Jones, M. Longo, D. Pellet, M. Perl, and F. Martin, Phys. Rev. Letters **13**, 59 (1964).

<sup>4</sup> J. Mathews and B. Deo, Phys. Rev. **143**, 1340 (1960).

<sup>5</sup> R. M. Heinz, O. E. Overseth, and M. H. Ross, Bull. Am. Phys. Soc. **10**, 19 (1965); R. M. Heinz, University of Michigan Technical Report No. 18, 1964 (unpublished).

<sup>6</sup> B. Deo and P. K. Patnaik, in Proceedings of Ninth Symposium on Cosmic Rays, Elementary Particles and Astrophysics, Bombay, 1965, p. 557 (unpublished).

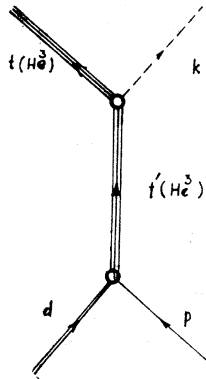


FIG. 2. Feynman diagram for  $p+d \rightarrow \text{He}^3 + \pi^0$  in direct channel with  $\text{He}^3$  pole.

reliably. All the same, some good results have already been obtained in this model<sup>4-6</sup> and we hope that this may also happen here. This optimism has motivated the present calculation.

In Sec. II we indicate the outline of our calculation. In Sec. III the  $pd$   $\text{He}^3$  vertex is obtained. Section IV deals with the discussion of the  $\text{He}^3\text{He}^3\pi^0$  coupling constant, and Sec. V deals with the numerical results. In the Appendix explicit expressions for scattering amplitudes are given with some details of calculation.

## II. MATRIX ELEMENTS

The invariant matrix element  $M$  can be written as

$$M = M_1 + M_2, \quad (2)$$

where  $M_1$  and  $M_2$  represent diagrams 1 and 2, respectively. The differential cross section is

$$\frac{d\sigma}{d\Omega} = \frac{1}{64\pi^2 W^2} \frac{p_f}{p_i} \frac{1}{(2S_1+1)(2S_2+1)} \sum |M|^2,$$

where  $p_i$  and  $p_f$  are initial and final three-momenta in the c.m. frame.  $S_1$  and  $S_2$  are spins of the initial particles and  $W$  is the c.m. energy. In calculating the scattering amplitude, the first thing that we must do is evaluate the  $\text{He}^3 d p$  vertex. This vertex is similar to the  $ndt$  vertex, which has been discussed by Blankenbekler *et al.*<sup>7</sup> Their result for the vertex is given as (Fig. 3)

$$\lambda \bar{u}(p)(\gamma \cdot \xi) \gamma_5 u(t), \quad (3)$$

where  $u(p)$  and  $u(t)$  are the spinors for proton and  $\text{He}^3$ . We shall use this vertex, but will calculate  $\lambda$  by Landau's<sup>8</sup> method with necessary modifications to include spin. Then we have

$$M_1 = \lambda g \bar{u}(t)(\gamma \cdot \xi) \gamma_5 (\gamma \cdot p' + m) \gamma_5 u(p) / (p'^2 - m^2), \quad (4)$$

$$M_2 = \lambda G \bar{u}(t) \gamma_5 (\gamma \cdot t' + M_t) \gamma_5 (\gamma \cdot \xi) u(p) / (t'^2 - M_t^2), \quad (5)$$

<sup>7</sup> R. Blankenbekler, M. L. Goldberger, and F. R. Halpern, *Nucl. Phys.* **12**, 629 (1959).

<sup>8</sup> L. D. Landau, *Zh. Eksperim. i Teor. Fiz.* **39**, 1856 (1960) [English transl.: *Soviet Phys.—JETP* **12**, 1294 (1961)]. See also M. Nauenberg, *Phys. Rev.* **124**, 2011 (1961); G. Barton, *Dispersion Techniques in Field Theory* (W. A. Benjamin, Inc., New York, 1965), p. 196.

where  $g$  is the pion-nucleon coupling constant and  $g^2/4\pi = 15$ .  $G$  is the  $\text{He}^3\pi$  coupling constant (Fig. 4).

## III. $\text{He}^3 pd$ VERTEX AND FORM FACTORS

The  $\text{He}^3 pd$  vertex is  $\lambda \bar{u}(p)(\gamma \cdot \xi) \gamma_5 u(t)$ . To determine  $\lambda$ , we calculate the differential cross section for<sup>8</sup> the process

$$p+d \rightarrow p+d. \quad (6)$$

Since the binding energy of  $\text{He}^3$  is very small, we write the resonance scattering formula<sup>9</sup>

$$d\sigma/d\Omega = \hbar^2/2\mu(E+B) \quad (7)$$

for the  $pd$  system. Here  $B$  is the binding energy of  $\text{He}^3$  ( $M_d + m - M_t$ ).  $M_t$  is the mass of  $\text{He}^3$ ,  $\mu$  is the reduced mass of the  $pd$  system and

$$E = W - M_d - m.$$

Now, calculating the contribution of Fig. 5 and comparing with Eq. (7) at the pole, we obtain

$$\lambda^2 = 4\pi(M_t/m^2)(\frac{1}{3}(m+M_d)B)^{1/2}. \quad (8)$$

Next we calculate the form factor for the same vertex. This form factor is due to the compositeness of the  $\text{He}^3$  and is proportional to the Fourier transform of the  $\text{He}^3$  wave function. The form factors approach unity when the particles are on the mass shell. Here we are concerned with  $\text{He}^3$  going to  $p+d$ . So the wave function should be the bound-state wave function of  $p$  and  $d$ . So far this wave function has not been obtained. For simplicity we take a Hulthén-type wave function

$$u(r) = (N/r)(e^{-\alpha(r-r_c)} - e^{-\beta(r-r_c)}), \quad \text{for } r > r_c \\ = 0, \quad \text{for } r < r_c \quad (9)$$

where  $\alpha = (2\mu B)^{1/2}$ ,  $B = M_d + m - M_t$ , and  $r_c$  is the hard-core radius. This wave function for large distances behaves exactly as a bound-state wave function of  $p$  and  $d$ .

To obtain  $N$  in Eq. (9) we imagine that  $M_t > M_d + m$ , so that  $\text{He}^3$  is unstable and decays into  $p+d$ . The matrix element describing this process is given by Eq. (3). If we represent the matrix element by  $T$ , the decay

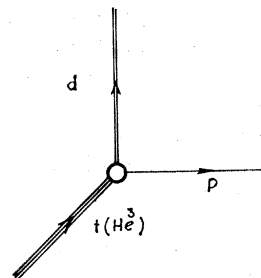


FIG. 3.  $\text{He}^3 pd$  vertex.

<sup>9</sup> L. D. Landau and R. M. Lifshitz, *Quantum Mechanics* (Addison-Wesley Publishing Co., Inc., Reading, Mass., 1958), p. 408.

rate is given by

$$\Gamma = \frac{1}{32\pi^2 M_t^2} \frac{1}{2S+1} \int \sum |T|^2 d\Omega. \quad (10)$$

Now we consider the  $\text{He}^3$  mass moving into its correct value below  $m+M_d$ . Then the  $\text{He}^3$  wave function changes from

$$\psi \sim N' e^{i\alpha r} / r \quad (11)$$

to

$$\psi \sim N' e^{-\alpha r} / r, \quad (12)$$

with

$$N' = [e^{\alpha r} / (4\pi)^{1/2}] N, \quad (13)$$

$$q^2 = [p'^2 - (M_t + M_d)^2][p'^2 - (M_t - M_d)^2] / 4M_t^2.$$

If we put the intermediate nucleon on the mass shell ( $p'^2 = m^2$ ), then  $q^2$  becomes  $-\alpha^2$ . Now Eq. (12) implies a decay rate

$$\Gamma = (4\pi q M_t / E_p E_d) |N'|^2. \quad (14)$$

Comparison of Eqs. (10) and (14) gives

$$N^2 = (\lambda^2 m / 3\pi) e^{-2\alpha r_c}, \quad (15)$$

where we have put  $M_t = 3m$  and  $M_d = 2m$ . On the other hand, we have

$$N^2 \int_{r_c}^{\infty} (e^{-\alpha(r-r_c)} - e^{-\beta(r-r_c)})^2 dr = 1, \quad (16)$$

so that we obtain a relation between  $\beta$  and  $r_c$

$$N^2 = 2\alpha\beta(\alpha+\beta) / (\beta-\alpha)^2 = (\lambda^2 m / 3\pi) e^{-2\alpha r_c}. \quad (17)$$

Finally, our form factor is given by

$$F(q^2) = (q^2 + \alpha^2) \phi(q^2),$$

$$\phi(q^2) = \frac{N(\beta^2 - \alpha^2)}{(q^2 + \alpha^2)(q^2 + \beta^2)} \left( \cos qr_c + \frac{\alpha\beta - q^2}{q(\alpha + \beta)} \sin qr_c \right), \quad (18)$$

and matrix elements

$$M_1 = \lambda g F(q^2) \bar{u}(t) (\gamma \cdot \xi) \gamma_5 \frac{\gamma \cdot p' + m}{p'^2 - m^2} \gamma_5 u(p), \quad (19)$$

$$M_2 = \lambda G F(q'^2) \bar{u}(t) \gamma_5 \frac{\gamma \cdot t' + M_t}{t'^2 - M_t^2} \gamma_5 (\gamma \cdot \xi) u(p), \quad (20)$$

$$q'^2 = [t'^2 - (M_d + m)^2][t'^2 - (M_d - m)^2] / 4M_t^2. \quad (21)$$

FIG. 4.  $\text{He}^3 \text{He}^3 \pi^0$  vertex.

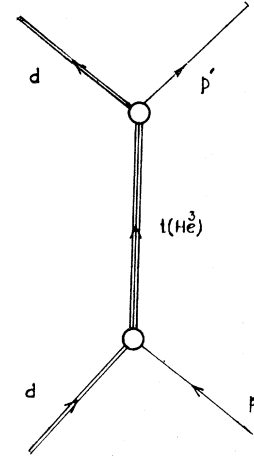
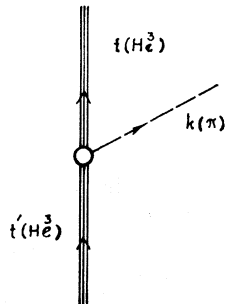


FIG. 5. Feynman diagram for  $p+d \rightarrow p+d$  in direct channel with  $\text{He}^3$  pole.

#### IV. $\text{He}^3 \text{He}^3 \pi^0$ COUPLING CONSTANT

To determine the value of  $G$ , we note that the triton and  $\text{He}^3$  form an isospin doublet. By analogy with the pion-nucleon interaction we can write down a  $\text{He}^3 \pi$  interaction of the form

$$G \bar{\psi}_H \gamma_5 \tau \cdot \phi \psi_H. \quad (22)$$

The pion is coupled to  $\text{He}^3$  through its coupling with the individual nucleons with the usual  $\gamma_5$  interaction

$$g \bar{\psi}_N \gamma_5 \tau \cdot \phi \psi_N, \quad (23)$$

where

$$\psi_H = \begin{pmatrix} \text{He}^3 \\ \text{H}^3 \end{pmatrix}, \quad \psi_N = \begin{pmatrix} p \\ n \end{pmatrix}.$$

Our next job is to correlate  $G$  with  $g$ . To do this we assume that the fictitious processes  $\text{He}^3 \rightarrow \text{He}^3 + \pi^0$  and  $\text{He}^3 \rightarrow \text{H}^3 + \pi^+$  are allowed. We calculate the decay widths from (22) and (23) and compare. However, there are some difficulties. Inside  $\text{He}^3$  there are two protons and one neutron. These two protons must obey the Pauli principle. When a neutron emits a  $\pi^0$ , its spin may or may not flip. But the proton spin cannot flip when a  $\pi^0$  is emitted. As a result, there will be a larger contribution to the non-spin-flip amplitude than to the spin-flip amplitude, and we shall not get the angular distribution expected from (22). So there must be some other constraints on the reaction so that we obtain the correct angular distribution. Here we discuss two possibilities of evaluating  $G$  without this difficulty.

(a) We assume that there exists some sort of correlation between the nucleons inside  $\text{He}^3$  such that when one proton spin flips, the other proton also does. Then the Pauli principle is not violated and there will not be any restriction on spin-flip or non-spin-flip amplitudes. Then we obtain

$$G^2 = g^2. \quad (24)$$

(b) As an alternative method of evaluation of  $G$ , we use the impulse approximation. Here we do not bother about spin-flip complications. Consider  $\text{He}^3 \pi^0$

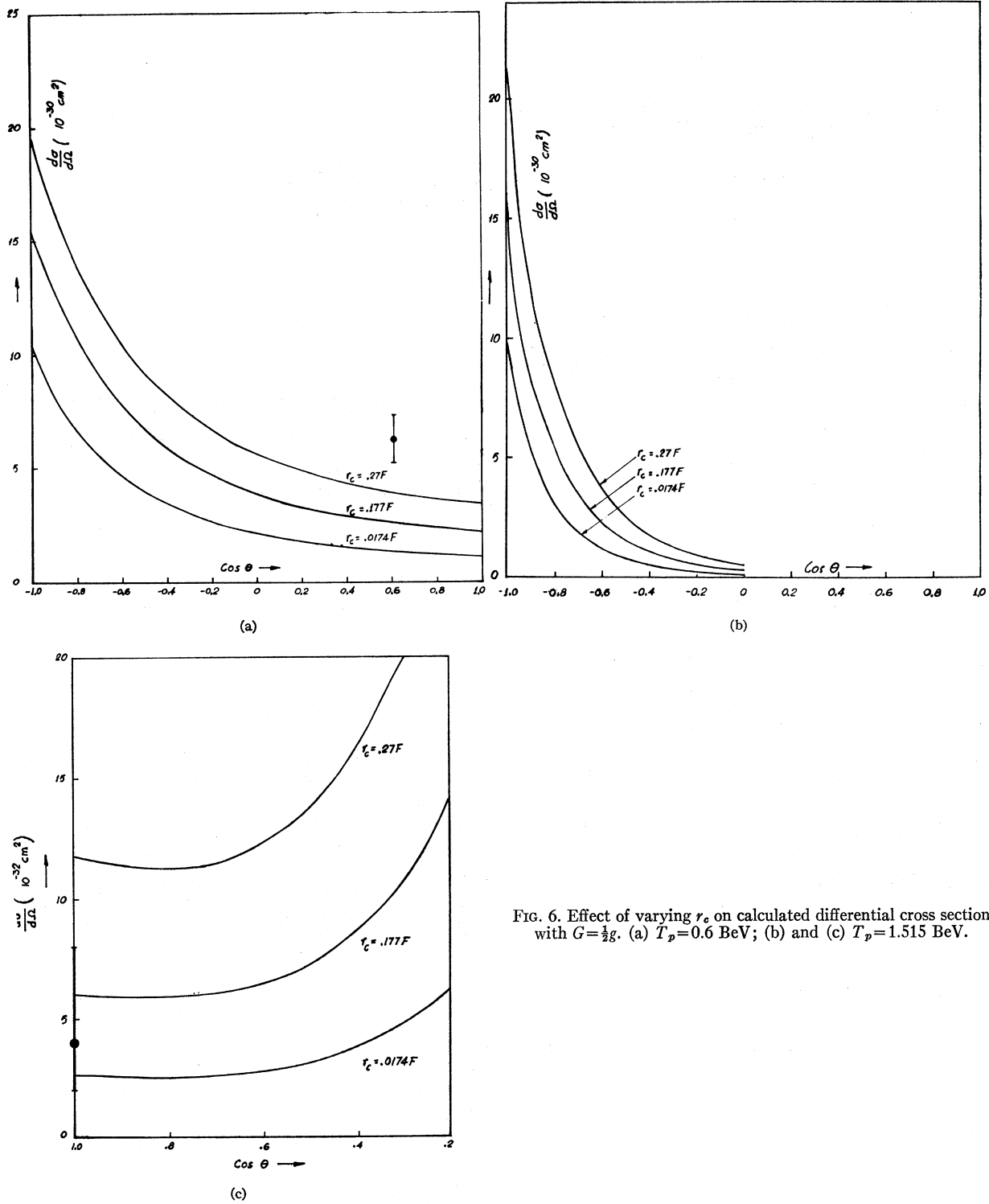


FIG. 6. Effect of varying  $r_c$  on calculated differential cross section with  $G = \frac{1}{2}g$ . (a)  $T_p = 0.6$  BeV; (b) and (c)  $T_p = 1.515$  BeV.

elastic scattering. At infinitely high energy we can write

$$\sigma(\text{He}^3 + \pi^0 \rightarrow \text{He}^3 + \pi^0) = 2\sigma(p + \pi^0 \rightarrow p + \pi^0) + \sigma(n + \pi^0 \rightarrow n + \pi^0). \quad (25)$$

At the limit of infinite energy the pole terms are most predominant and we get contributions to the total cross section only from two points:  $\cos \theta = \pm 1$ , corresponding to  $t$ - and  $u$ -channel poles. Here we make an assumption that  $t$ - and  $u$ -channel contributions do

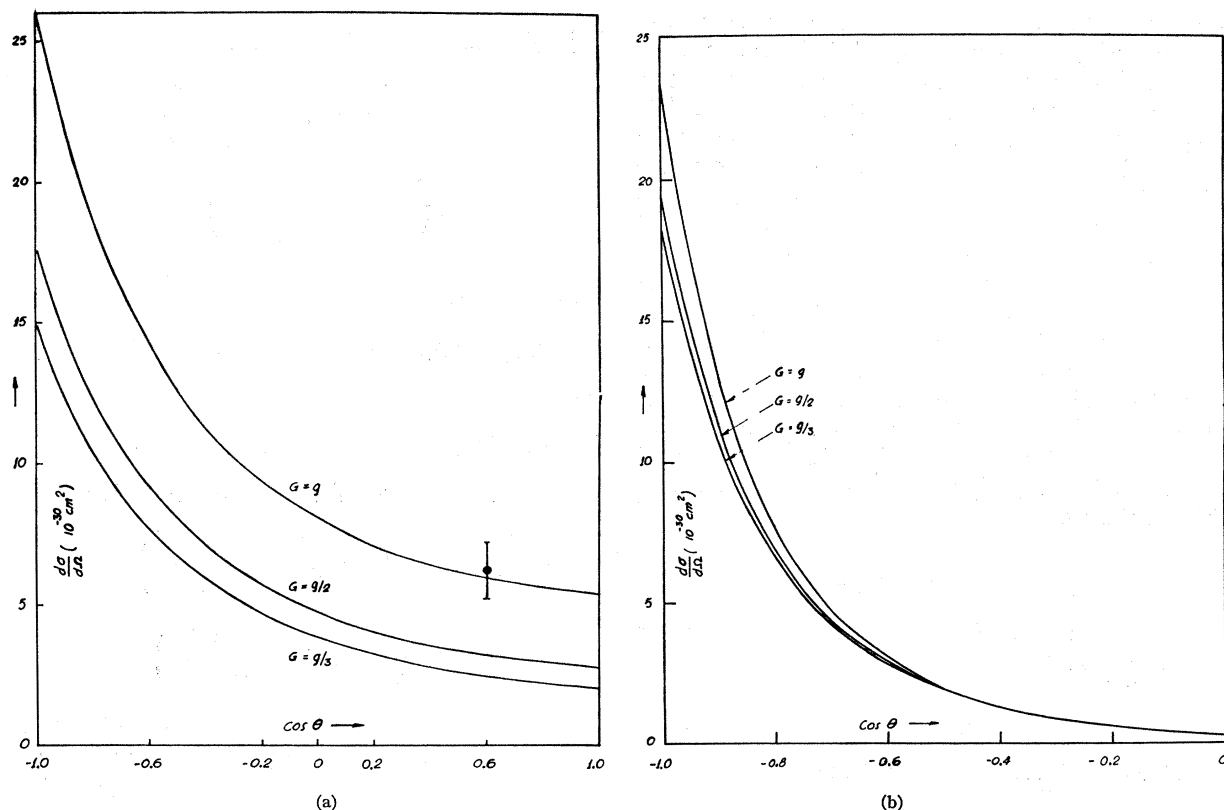


FIG. 7. Effect of varying  $G$  on calculated differential cross section with  $r_c = 0.23$  F. (a)  $T_p = 0.6$  BeV; (b)  $T_p = 1.515$  BeV.

not mix together. This means that  $t$ - and  $u$ -channel contributions can be equated separately. Then we get

$$G^4 = 3g^4. \quad (26)$$

Now we have obtained two values for  $G$ :  $g$  and  $1.3g$ . The first result is obtained with an assumption that is plausible but cannot be verified experimentally. The second result is a rough estimate based on a valid approximation. However, one thing that we conclude is that  $G$  and  $g$  are of the same order of magnitude. In actual calculations we shall use  $G$  as a parameter and vary it in the neighborhood of  $g$ .

## V. NUMERICAL RESULTS

In this section we report the numerical calculations, using formulas of Secs. II and III and the Appendix. The numerical calculations were done by an IBM 7044 computer at the Indian Institute of Technology, Kanpur.

In Fig. 6(a) we have plotted the differential cross section with  $T_p = 0.6$  BeV,  $G = \frac{1}{3}g$ , and giving  $r_c$  three different values.  $g$  is the pion-nucleon coupling constant. In Figs. 6(b) and 6(c) we repeat this with  $T_p = 1.515$  BeV. We obtain the experimental result of Ref. 1 for the two different values of  $r_c$ , while that of Ref. 2 is slightly more than the calculated value. For  $T_p = 1.515$

BeV the change in angular distribution is very rapid. For  $T_p = 0.6$  BeV the variation is much slower. At 1.515 BeV the scattering is mostly in the backward direction ( $\theta_{c.m.} = 180^\circ$ ) and the scattering at forward angles decreases very rapidly.

In Figs. 7(a) and 7(b) we keep  $r_c$  fixed at 0.23 F and see the effect of varying  $G$  on the differential cross section. For  $T_p = 0.6$  BeV the variation is significant,

TABLE I. Differential cross section for proton kinetic energies 0.6 and 1.515 BeV at angles  $52^\circ$  and  $0^\circ$ , respectively.

| $G$                  | $r_c$<br>(F) | $\frac{d\sigma}{d\Omega}$   | $\frac{d\sigma}{d\Omega}$  |
|----------------------|--------------|---|--|
|                      |              | $T_p = 0.6$ BeV<br>( $10^{-30}$ cm $^2$ )<br>$\theta_{c.m.} = 52^\circ$ | $T_p = 1.515$ BeV<br>( $10^{-32}$ cm $^2$ )<br>$\theta_{c.m.} = 0^\circ$ |
| $g$                  | 0.11         | 3.53  | 10   |
|                      | 0.177        | 4.72  | 15   |
|                      | 0.23         | 5.95  | 21   |
|                      | 0.27         | 7.2   | 28   |
|                      | 0.3          | 8.40  | 37   |
| $\frac{1}{3}g$       | 0.11         | 1.9   | 4  |
|                      | 0.177        | 2.5   | 6  |
|                      | 0.23         | 3.2   | 8  |
|                      | 0.27         | 3.7   | 11   |
|                      | 0.3          | 4.5   | 15   |
| Experimental result: |              | $6.1 \pm 2$   | $4.0_{-2}^{+4}$  |

whereas for  $T_p=1.515$  BeV the variation is very small but not negligible. From the graph it looks as though the effect is negligible. This is because the cross section in the forward direction ( $\theta_{e.m.}=0^\circ$ ) is itself negligible compared to that in the backward direction, so that the variation is also negligible. However, compared to the values of the differential cross section at  $0^\circ$ , the variation is quite significant. This can be very easily observed from Table I, where we have tabulated two sets of values—one for  $T_p=0.6$  BeV and  $\theta_{e.m.}=52^\circ$  and the other for  $T_p=1.515$  BeV and  $\theta_{e.m.}=0^\circ$ . We have taken two values of  $G$ , i.e.,  $g$  and  $\frac{1}{2}g$ , and  $r_c$  is given several values. Although we find that our results are of the same order of magnitude as those of Refs. 1 and 2, we feel that the experimental value for  $T_p=1.515$  BeV should have been slightly more, or that for  $T_p=0.6$  BeV should have been slightly less, to give perfect agreement with our theory.

#### ACKNOWLEDGMENT

The author is thankful to Professor B. B. Deo for encouragement.

#### APPENDIX

We have the invariant matrix element

$$M = M_1 + M_2,$$

$$\sum |M|^2 = \sum |M_1|^2 + \sum |M_2|^2 + \sum (M_1^\dagger M_2 + M_2^\dagger M_1),$$

$$\sum |M_1|^2 = (A + B + C)F^2(q^2)/(p'^2 - m^2)^2,$$

with

$$A = 12\lambda^2 g^2 [2(p \cdot p' - m^2)(p' \cdot t + mM_t) - (p \cdot t + mM_t)(p'^2 - m^2)],$$

$$B = 4\lambda^2 g^2 (d \cdot t / M_d^2) [2(d \cdot p')(p \cdot p' - m^2) - (p \cdot d)(p'^2 - m^2)],$$

$$C = -4\lambda^2 g^2 [2(p' \cdot t)(p \cdot p' - m^2) - (p \cdot t)(p'^2 - m^2)];$$

$$\begin{aligned} \sum |M_2|^2 = & 4\lambda^2 G^2 \left[ -3\mu^2 (p \cdot t + mM_t) \right. \\ & + 4(k \cdot t) \left( -p \cdot k + \frac{(d \cdot p)(d \cdot k)}{M_d^2} \right) \\ & \left. - 2\mu^2 \left( -p \cdot t + \frac{(d \cdot p)(d \cdot t)}{M_d^2} \right) + 6(k \cdot t)(p \cdot k) \right] \\ & \times F(q'^2)/(l'^2 - M_t^2)^2, \end{aligned}$$

$$\begin{aligned} \sum (M_1^\dagger M_2 + M_2^\dagger M_1) \\ = 2\lambda^2 g G F(q^2) F(q'^2) (X + Y + Z) / (p'^2 - m^2)(l'^2 - M_t^2), \end{aligned}$$

with

$$\begin{aligned} X = & -12 \left[ (p \cdot p' - m^2)(l \cdot l' - M_t^2) - (p \cdot t + mM_t) \right. \\ & \left. \times (p' \cdot l' + mM_t) + (p \cdot l' + mM_t)(p' \cdot t + mM_t) \right], \end{aligned}$$

$$\begin{aligned} Y = & -8 \left[ (l \cdot l' - M_t^2) \left( -p \cdot p' + \frac{(d \cdot p)(d \cdot p')}{M_d^2} \right) \right. \\ & - (p \cdot t + mM_t) \left( -p \cdot p' + \frac{(d \cdot p)(d \cdot p')}{M_d^2} \right) \\ & \left. + (p \cdot l' + mM_t) \left( -p' \cdot t + \frac{(d \cdot p')(d \cdot t)}{M_d^2} \right) \right], \end{aligned}$$

$$\begin{aligned} Z = & 8 \left[ (l \cdot l' - M_t^2) \left( -p \cdot p' + \frac{(d \cdot p)(d \cdot p')}{M_d^2} \right) \right. \\ & - (p' \cdot t + mM_t) \left( -p \cdot p' + \frac{(d \cdot p)(d \cdot p')}{M_d^2} \right) \\ & \left. + (p' \cdot l' + mM_t) \left( -p \cdot t + \frac{(d \cdot p)(d \cdot t)}{M_d^2} \right) \right]. \end{aligned}$$

All these quantities were calculated by the usual techniques of trace and projection operators. For the deuteron polarizations we had

$$\begin{aligned} \sum |\xi|^2 &= -3, \\ \sum (\xi \cdot A)(\xi \cdot B) &= -(A \cdot B) + (d \cdot A)(d \cdot B) / M_d^2, \\ d \cdot \xi &= 0. \end{aligned}$$